Expression and Regulation of Epithelial Na^+ Channels by Nucleotides in Pleural Mesothelial Cells

Hong-Guang Nie[1,4], Torry Tucker[1], Xue-Feng Su[2], Tao Na[3], Ji-Bin Peng[3], Peter R. Smith[2], Steven Idell[1], and Hong-Long Ji[1]

[1]Department of Biochemistry, Texas Lung Injury Institute, University of Texas Health Science Center at Tyler, Tyler, Texas; [2]Department of Physiology and Biophysics, and [3]Department of Medicine, University of Alabama at Birmingham, Birmingham, Alabama; and [4]Department of Pharmacology, School of Pharmaceutical Sciences, China Medical University, Shenyang, China

Pleural effusions are commonly clinical disorders, resulting from the imbalance between pleural fluid turnover and reabsorption. The mechanisms underlying pleural fluid clearance across the mesothelium remain to be elucidated. We hypothesized that epithelial Na^+ channel (ENaC) is expressed and forms the molecular basis of the amiloride-sensitive resistance in human mesothelial cells. Our RT-PCR results showed that three ENaC subunits, namely, α, β, γ, and two δ ENaC subunits, are expressed in human primary pleural mesothelial cells, a human mesothelioma cell line (M9K), and mouse pleural tissue. In addition, Western blotting and immunofluorescence microscopy studies revealed that α, β, γ, and δ ENaC subunits are expressed in primary human mesothelial cells and M9K cells at the protein level. An amiloride-inhibitable short-circuit current was detected in M9K monolayers and mouse pleural tissues when mounted in Ussing chambers. Whole-cell patch clamp recordings showed an ENaC-like channel with an amiloride concentration producing 50% inhibition of 12 μM in M9K cells. This cation channel has a high affinity for extracellular Na^+ ions (K_m: 53 mM). The ion selectivity of this channel to cations follows the same order as ENaC: $Li^+ > Na^+ > K^+$. The unitary Li^+ conductance was 15 pS in on-cell patches. Four ENaC subunits form a functional Na^+ channel when coinjected into *Xenopus* oocytes. Furthermore, we found that both forskolin and cGMP increased the short-circuit currents in mouse pleural tissues. Taken together, our data demonstrate that the ENaC channels are biochemically and functionally expressed in human pleural mesothelial cells, and can be up-regulated by cyclic AMP and cyclic GMP.

Keywords: M9K mesothelioma cells; Ussing chamber; protein kinase A; protein kinase G; human primary mesothelial cells

Mesothelial cells are specialized epithelial cells that line the serous cavities (pleural, pericardial, and peritoneal) and internal organs (1). The mesothelium was first described 175 years ago, but only over the past 20 years has it been realized that mesothelial cells play a critical role in maintaining the integrity and function of the serosal cavities (2). Recently, *in vivo* and *in vitro* experimental evidence has shown that the mesothelium is less permeable than previously believed, being provided with permeability characteristics similar to those of epithelium (3–5). A key function of the mesothelium is its active role in transerosal transport—in particular, cavity fluid turnover and reabsorption. Compelling evidence indicates that mesothelial cells actively transport fluid and electrolytes across the serosa (6, 7).

CLINICAL RELEVANCE

This study shows, for the first time, that epithelial sodium channels are expressed in pleural mesothelial cells and govern ion transport.

The epithelial sodium channel (ENaC), which participates in Na^+ movement across the apical membrane of epithelial cells, has been cloned and characterized (8, 9). Five ENaC subunits have been cloned to date, namely, α, β, γ, δ, and ε ENaC (10). The biophysical properties of ENaC channels depend on subunit composition. α-Like conducting subunits, including α, δ, and ε subunits, can form a channel sharing identical properties to the channels composed of one of the conducting subunits plus a βγ ENaC mixture. By contrast, αβ and αγ ENaC channels display variant amiloride sensitivities, conductances, and Na^+ permeabilities (10, 11). The single-channel conductance of αβγ ENaC expressed in *Xenopus* oocytes is 4- to 6-picoseimens (pS), and is highly selective for Na^+ over K^+ ions (10, 12–14). The diuretic amiloride inhibits Na^+ transport when added to the solution bathing the apical plasma membrane, at a concentration less than 10^{-6} M (15, 16).

Indirect evidence supporting the presence of amiloride-sensitive Na^+ channels in human and sheep peritoneal membrane has been presented (17, 18). A significant increment in the transmesothelial electrical resistance was observed after addition of amiloride, indicating an amiloride-sensitive ion transport pathway. It has been proposed that this ion transport system may play a role in the ultrafiltration process and Na^+ removal during peritoneal dialysis. Interestingly, the amiloride-sensitive electrical resistance of the diaphragmatic parietal pleura is significantly higher than that of the costal parietal pleura, suggesting that the costal pleura is more permeable than the diaphragmatic pleura (19). It is noteworthy that amiloride exerted its action only on the apical side, but not on the basolateral side. By comparison with polarized epithelial cells, it is conceivable that ENaC proteins are expressed on the mesothelial surfaces that line the peritoneal cavity.

Very recently, Jiang and colleagues (20) examined the amiloride-sensitive fluid transport pathway in pleura *in vivo*. The β_2-adrenergic receptor agonist, terbutaline, increased pleural isosmolar fluid absorption, which was inhibited by amiloride. Terbutaline has long been used clinically to effectively ameliorate pulmonary edema by up-regulating ENaC activity, and thereby expediting edematous liquid clearance (21, 22). These observations support the scenario that ENaC channels are functionally expressed in pleural tissues and contribute to pleural fluid reabsorption. However, our understanding of the cellular distribution of ENaC and its biophysical properties in mesothelial cells is still rudimentary.

In the present study, we have examined ENaC expression in human and mouse mesothelial cells. We detected the expression of α, β, γ, and δ ENaC subunits at the mRNA and protein levels in

(*Received in original form April 30, 2008 and in final form September 7, 2008*)

This work was supported by NIH grants HL 87017 (H.-L.J.) and PO1 HL076406 (S.I.).

Correspondence and requests for reprints should be addressed to Hong-Long (James) Ji, M.D., Department of Biochemistry, Texas Lung Injury Institute, The University of Texas Health Science Center at Tyler, 11937 U.S. Highway 271, Tyler, TX 75708. E-mail: James.Ji@uthct.edu

Am J Respir Cell Mol Biol Vol 40. pp 543–554, 2009
Originally Published in Press as DOI: 10.1165/rcmb.2008-0166OC on October 16, 2008
Internet address: www.atsjournals.org

M9K cells, a human pleural mesothelioma cell line, and mouse pleural tissues (23). An amiloride-sensitive, ENaC-like short-circuit current (I_{sc}) was recorded in mouse pleural tissues and confluent M9K monolayers mounted in an Ussing chamber (23). Furthermore, an amiloride-sensitive, highly Na^+-permeable channel was characterized using whole-cell and single-channel patch clamp techniques. These results clearly demonstrate that the ENaC channel, composed of four subunits, is both biochemically and functionally expressed in mesothelial cells.

MATERIALS AND METHODS

Cell Culture

NCI-H441 cells were obtained from the American Type Culture Collection. The human pleural mesothelial M9K cell line and human primary pleural mesothelial cells were provided by Dr. Steven Idell (University of Texas Health Center at Tyler). The human pleural mesothelial cells were obtained from pleural effusions of patients with congestive heart failure under the auspices of a protocol approved by the Human Subjects Institutional Review Board of the University of Texas Health Science Center at Tyler. H441 and human primary mesothelial cells were grown in RPMI medium (American Type Culture Collection), supplemented with 10% FBS, and antibiotics. M9K cells were grown in Medium 199 (Invitrogen, Carlsbad, CA) supplemented with 10% FBS, penicillin (100 U/ml), and streptomycin (100 μg/ml). Cells were seeded in 75-cm^2 flasks and incubated in a humidified atmosphere of 5% CO_2–95% O_2 at 37°C. For patch clamp studies, cells were lifted using 0.25% trypsin and 0.53 mM EDTA (Sigma, St. Louis, MO), then seeded at a density of 1×10^6 cells/ml on round coverslips (8 mm; WPI, Sarasota, FL) situated in 24-well culture plates. Cells were grown in the same medium supplemented with 200 nM dexamethasone to facilitate Na channel differentiation; the medium was replaced every other day. For immunofluorescence studies, cells were seeded on transwell permeable support filters (Corning Costar, Lowell, MA) and maintained until confluent monolayers were formed. Serum-free RPMI medium containing 200 nM dexamethasone was applied to each well 24 hours before fixation and harvest for Western blot studies. To obtain confluent monolayers for Ussing chamber studies, cells were plated at a density of approximately 5×10^6 cells/cm^2 onto Costar transwell inserts (model 3,470) and grown in the Medium 199 supplied with dexmathasone (200 nM). Medium was replaced every other day for liquid–liquid interface culture. The transmesothelial resistance (Rt) was greater than 500 MΩ in 7–10 days.

RT-PCR

Confluent M9K and human primary mesothelial cells were scraped into ice-cold PBS. Cells were snap frozen in a dry ice–methanol mixture and stored at −80°C after pelleting in a microcentrifuge. Mouse parietal pleural tissues were surgically isolated from fully anesthetized BALB/c male mice (Jackson Laboratory, Bar Harbor, ME) anesthetized by intraperitonal injection of ketamine (100 mg/kg) and xylazine (8.5 mg/kg). Excised pleural tissues were washed by ice-cold PBS and stored at −80°C. Total RNA was extracted using TRIzol reagent (Invitrogen) according to the manufacturer's instructions. RNA was dissolved in RNase-free water and stored at −80°C. RNA was treated with DNase I (RNase-free; Ambion, Austin, TX), according to manufacturer's protocol, to eliminate potentential genomic DNA contamination. RNA was then extracted by acidic phenol-chloroform (pH 4.0; Ambion) to inactivate DNase I. RNA concentration was assessed by spectrophotometry at 260 nm. RNA quality was confirmed by running 5 μg of total RNA from each preparation on a 1.2% denatured agarose gel. The specific oligonucleotide primers for the RT-PCR analysis of the α, β, δ, and γ ENaC subunits were as follows: α ENaC, 5′-AAC AAA TCG GAC TGC TTC TAC-3′ (sense), 5′-AGC CAC CAT CAT CCA TAA A-3′ (antisense); β ENaC, 5′-GGG ACC AAA GCA CCA AT-3′ (sense), 5′-CAG ACG CAG GGA GTC ATAG-3′ (antisense); δ ENaC, 5′-CGA AGC ATG GAC GGG AGA ATG-3′ (sense), 5′-GGT GCC AGT GAC GCT CAA AGA-3′ (antisense); and γ ENaC, 5′-GCA CCG TTC GCC ACC TTC TA-3′ (sense), 5′-AGG TCA CCA GCA GCT CCT CA-3′ (antisense). Sequence accession numbers in GenBank are 38,197,484, 4,506,816, 34,101,281, and 42,476,332 for the α, β, δ, and γ subunits, respectively. The corresponding product sizes are 406 bp (α), 440 bp (β), 325 bp and 418 bp (δ), and 456 bp (γ). The oligonucleotide primers for α, β, δ, and γ ENaC were synthesized by Sigma Genosys, and used at a final concentration of 0.6 μM. RT-PCR was performed using the OneStep RT-PCR kit (Qiagen, Valencia, CA) in a Mastercycler gradient thermocycler (Eppendorf Scientific, Westbury, NY). Total RNA (1 μg) was used as a template for each reaction. Reverse transcription was performed using a single cycle of 50°C for 30 minutes. This was followed by a single cycle of 95°C for 15 minutes to inactivate the reverse transcriptase, while activating the HotStart TaqDNA polymerase, and then 30 cycles of 94°C for 0.5 minutes, 60°C to approximately 66°C for 1 minute, 72°C for 1.5 minutes, followed by a single 10-minute cycle at 72°C for extension. Annealing temperatures are different for α, β, δ, and γ (α 60°C, β 60°C with 5× Q buffer, δ 66°C, γ 65°C with 5× Q buffer). RT-PCR products were electrophoresed on a 1.5% agarose gel using 100-bp PCR markers (Promega, Madison, WI) as a standard to determine the molecular size. Products of the predicted molecular size were excised and purified from the gel using the QIAquick gel extraction kit (Qiagen) and subcloned into the PCR-2.1 vector (Invitrogen). Positive clones were selected by blue/white screening and followed by digestion with EcoRI (Promega) to verify incorporation of insert of the correct size. Authenticity of PCR products in the pCR2.1 vector were verified by automated DNA sequencing (DNA Sequencing Core, University of Alabama at Birmingham, Birmingham, AL).

Western Blot Assays

To identify the subcellular location of ENaC proteins in confluent M9K cells, cells grown on filters were incubated with membrane-impermeable biotin added to the luminal or basolateral compartment. Biotinylated cells were then washed and lysed for immunoblotting assay. After separation by SDS-PAGE (6% gels), proteins were transblotted onto polyvinylidene fluoride membrane (Bio-Rad, Hercules, CA). After a 1-hour incubation in a blocking solution containing 20 mM Tris-Cl (pH 7.5), 0.5 M NaCl, 5% nonfat dried milk, the membrane was incubated with anti-ENaC antibodies in an antibody buffer containing 20 mM Tris-Cl (pH 7.5), 0.5 M NaCl, 0.1% Tween 20, and 0.2% nonfat dried milk at 4°C overnight. Incubation at room temperature for 30 minutes was used for secondary antibodies. Three 5-minute washes in washing buffer (20 mM TrisCl [pH 7.5], 0.5 M NaCl, and 0.1% Tween 20) were applied after each antibody reaction. Antibodies used in this study included a goat polyclonal antibody directed against a region in the C terminus of human α ENaC (α hENaC), a rabbit polyclonal antibody directed against amino acids 81–310 of δ hENaC, and a goat antibody directed against a peptide derived from γ hENaC (all purchased from Santa Cruz Biotechnology, Santa Cruz, CA). ECL kit (Amersham, Piscataway, NJ) was used to develop the image. Antibodies against ENaC subunits were diluted 1:5,000 when used.

Indirect Immunofluorescence and Confocal Microscopy

Cells on filters or coverslips were fixed in 3% formaldehyde (EM Sciences, Gibbstown, NJ) for 45 minutes, followed by incubation with 0.5% Triton X-100 for 3 minutes Nonspecific protein binding sites were blocked with 3% BSA. Cells were incubated with anti-α, -β, -γ, and -δ ENaC polyclonal antibodies from Santa Cruz Biotechnology (Santa Cruz, CA), Chemicon (Billerica, MA), and ABR (Rockford, IL) at 20 μg/ml for 2 hours at room temperature. Cells incubated with nonimmune IgG served as negative controls. The cells were then incubated with 10 μg/ml Alexa Fluor 488 goat anti-rabbit IgG (heavy + light) (Invitrogen) for 2 hours at room temperature in darkness. Cell nuclei were stained with 300 nM 4′,6-diamidino-2-phenylindole (Invitrogen) for 5 minutes. Cells grown on filters or coverslips were finally mounted in Vectorshield mounting media H-1000 (Vector Laboratories, Burlingame, CA) and sealed with clear nail polish. Images were photographed with a high-resolution camera (model S97809; Olympus America, Inc., Center Valley, PA) attached to an inverted epifluorescence microscope (model BX50; Olympus). The digital camera was controlled by PictureFrame software, version 2.3 (Olympus). Side view images were digitized using a confocal microscopy, as described previously (24). Merged images were processed using Photoshop CS3 extended (Adobe Corp., San Jose, CA).

Ussing Chamber Assay

The use of animals for this study was approved by the Animal Research Committee, University of Texas Health Science Center at Tyler. Mouse parietal pleural tissues were surgically isolated from fully anesthetized BALB/c male mice, as described above. Excised pleural tissues were kept in the physiological salt solution (117 mM NaCl, 25 mM $NaHCO_3$, 4.7 mM KCl, 1.2 mM $MgSO_4$, 1.2 mM KH_2PO_4, 2.5 mM $CaCl_2$, 11 D-glucose, pH 7.3 $\sim$ 7.4) (25) before mounting in the Ussing chambers (Physiologic Instruments, San Diego, CA). Osmolarity of the bath solution was between 290 and 300 mOsm. The transmesothelial I_{sc}s were measured with 3 M KCl, 4% agar bridges placed 3 mm on either side of the membrane, which were connected on either side to Ag-AgCl electrodes. The samples were bathed on both sides with the above physiological salt solution, bubbled continuously with a 95% O_2–5% CO_2 gas mixture. The temperature of bath solutions (37°C) was maintained by using a temperature-controlled water bath for at least 30 minutes before the measurement of I_{sc}. M9K monolayers or mouse pleural tissues were short-circuited to 0 mV, and I_{sc} was measured with a VCC-MC8 voltage clamp amplifier (Physiologic Instruments). A 10-mV pulse of 1-second duration was imposed every 10 seconds to monitor Rt and I_{sc}. The experimental solution bathing the surface of the pleura that ordinarily faces the pleural liquid *in vivo* is referred to as the mucosal solution, whereas the solution bathing the surface normally exposed to the blood supply is referred to as the serosal solution. Similarly, the mesothelial cell membranes facing the pleural liquid or blood side is referred to as the apical or basolateral membrane, respectively. After the establishment of steady-state values of I_{sc} and Rt, specific activators or channel inhibitors were added to the mucosal solution of parietal pleura or to the apical side of M9K monolayers, and I_{sc} and Rt were measured continuously until new steady-state values were reached. The amiloride stock solution (50 mM) was dissolved in DMSO.

For recording I_{sc} in basolateral membrane permeabilized monolayers, 100 μM amphotericin B was added to the basolateral side of the Ussing chamber after the basal I_{sc} level was obtained. We established a 145:25-mM Na^+ gradient (apical to basolateral) across the monolayers by replacing 120 mM N-methyl-D-glucamine, an impermeant cation. Basolateral membrane permeabilization equilibrated intracellular Na^+ concentration with that in the basolateral compartment. Under these conditions, I_{sc} is the result of passive Na^+ flux through apical Na^+ conductive pathways, down the Na^+ concentration gradient from the apical to the basolateral side (26, 27). When the I_{sc} had attained its maximum value, the amiloride sensitivity was determined by adding 1 $\sim$ 1,000 μM amiloride to the apical compartment from lower to higher concentrations. Data were collected using the Acquire and Analyze program,version 2.3 (Physiologic Instruments).

Oocyte Preparation and Voltage Clamp Analysis

Oocytes were surgically removed from appropriately anesthetized adult female *Xenopus laevis* (Xenopus Express, Brooksville, FL) and cRNAs for α, β, γ, and δ hENaC were prepared as described previously (10). Briefly, the ovarian tissue was removed from frogs under anesthesia by ethyl 3-aminobenzoate methanesulfonate salt (Sigma) through a small incision in the lower abdomen. Follicle cells were removed and digested in Oocyte Ringer solution 2 (OR-2) calcium-free medium (82.5 mM NaCl, 2.5 mM KCl, 1.0 mM $MgCl_2$, 1.0 mM Na_2HPO_4, and 10.0 mM HEPES, pH 7.5) with the addition of 2 mg/ml collagenase (Roche, Indianapolis, IN). Defolliculated oocytes were cytosolically injected with hENaC cRNAs (25 ng) per oocyte in 50 nl of RNase-free water with a ratio of 1α:1β:1γ:1δ subunit, and incubated in half-strength L-15 medium at 18°C. Cells without cRNA injection served as control. The two-electrode voltage clamp technique was used to record whole-cell currents 48 hours after injection. Oocytes were impaled with two electrodes filled with 3 M KCl, having resistances of 0.5–2.0 MΩ. A TEV-200 voltage clamp amplifier (Dagan, Minneapolis, MN) was used to clamp oocytes with concomitant recording of currents. Two reference electrodes were connected to the bath. The continuously perfused bathing solution was ND96 medium (96.0 mM NaCl, 1.0 mM $MgCl_2$, 1.8 mM $CaCl_2$, 2.5 mM KCl, and 5.0 mM HEPES, pH 7.5). Experiments were controlled by pCLAMP 10.1 software (Molecular Devices, Sunnyvale, CA), and currents at −40, −100, and +80 mV were continuously monitored with an interval of 10 seconds. The current–voltage (I-V) relationships were acquired by stepping the holding potential in 20-mV increments from −120 to +80 mV after the monitoring currents were stable, before and after the application of amiloride to the perfusate. Data were sampled at the rate of 200 Hz and filtered at 500 Hz.

Patch Clamp Recordings

Immediately before each experiment, a coverslip bearing M9K cells was removed from the culture plate and put into a recording chamber, which was mounted on the stage of an inverted fluorescent microscope (DM IRB; Leica, Bannockburn, IL). For whole-cell patch clamp recording, cells were continuously perfused with external solution containing 140 mM NaCl, 1.8 mM $CaCl_2$, 1 mM $MgCl_2$, and 10 mM HEPES (pH 7.2) (28). Pipettes were made from capillary glass (WPI) with a P-97 micropipette puller (Sutter, Novato, CA). They were back-filled with internal solution composed of 100 mM K-gluconate, 40 mM KCl, 2 mM $MgCl_2$, 0.5 mM $CaCl_2$, 2 mM K_2ATP, 4 mM EGTA, and 10 mM HEPES (pH 7.2). The pipette resistance varied from 5 to 10 MΩ when filled with this internal solution. Offset potential was corrected just before a gigaohm seal formation. Series resistance and capacitance transients were compensated with an Axopatch 200B amplifier (Molecular Devices). Currents were digitized with a Digidata 1440A converter (Molecular Devices), filtered through an internal four-pole Bessel filter at 1 kHz, and sampled at 2 kHz. Inward and outward whole-cell currents were elicited by employing a step-pulse protocol from −100 to +100 mV in 10-mV increments every 10 seconds for 500 milliseconds duration from a holding potential of −40 mV. Steady-state currents were averaged between 100 and 200 milliseconds. Cells with a similar diameter were selected for recordings, and only those cells with stable baseline currents were included in the results. Amiloride sensitivity was evaluated by applying various concentrations to the bath (1 μM to 1 mM).

To examine the cation permeability of the native channel in M9K cells, NaCl in the external solution was replaced with equivalent amounts of LiCl or KCl salts. For the Na^+ affinity studies, M9K cells were perfused with solutions containing different external Na^+ concentrations in an order of 0, 10, 30, 60, 100, and 140 mM. Osmolarity of all solutions was balanced with N-methyl-D-glucamine (between 290 and 300 mOsm). The permeability ratios between Na^+ and other cations (P_{Na}:P_X) were calculated using the differences in reversal potentials obtained when the same cell was continuously perfused with Na^+-, Li^+-, or K^+-rich solutions:

$$\Delta E_{rev} = E_{rev}^{Na} - E_{rev}^{x} = \frac{RT}{zF} \ln \frac{P_{Na}[Na]_{out}}{P_X[X]_{out}}$$

where E_{rev} stands for the reversal potential for Na^+ or test cations (X) in the bath solution, z is the valence of the test cation, R is the gas constant, T is the absoute temperature, and F is Faraday's constant.

For single-channel recordings, the cell-attached mode was used. The pipettes were back-filled with an external solution consisting of 140 mM LiCl, 3 mM $MgCl_2$, and 10 mM HEPES (pH 7.4) (29). Pipette resistance, when filled with this solution, was $\sim$ 20 MΩ. The offset potential was corrected. To neutralize resting membrane potential (V_m), cells were perfused with a solution containing 134 mM K^+-gluconate, 10 mM KCl, 5 $MgCl_2$, 10 mM HEPES, and 5.5 mM glucose (pH 7.4) (30). Patch potential was calculated as: $V_{patch} = -V_{pipette}$, where $V_{pipette}$ is the applied potential. Data were sampled at 1–2 kHz and filtered at 0.3 kHz. A 50-Hz low-pass digital filter was applied for subsequent analysis.

Statistical Analysis

All results are presented as means (± SE). Amiloride-sensitive currents are defined as the difference between the total current and the amiloride-resistant current. One-way analysis of mean and variance computation was used to analyze data with unequal variance between each group. A probability level of 0.05 was considered significant.

RESULTS

Expression of ENaC mRNA in Human Mesothelial Cells

To examine α, β, γ, and δ ENaC expression in human and mouse mesothelial cells and tissues at the mRNA level, we performed

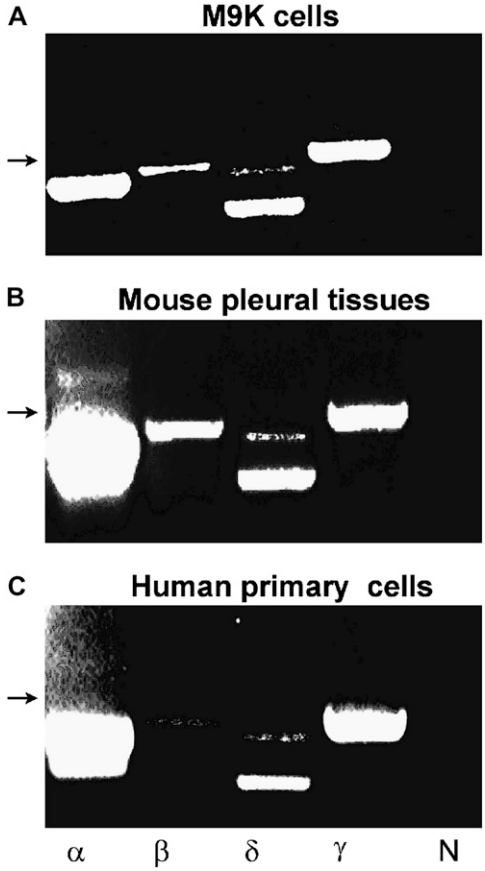

Figure 1. RT-PCR analysis of α, β, γ, and δ epithelial Na channel (ENaC) mRNA expression in human pleural mesothelial cells and mouse pleural tissues. The expression pattern of ENaC subunits was confirmed with three independent experiments using the OneStep RT-PCR kit. The lanes from *left* to *right* represent α, β, δ, and γ ENaC subunits (α, β, δ, γ) and negative control (*N*). *Arrows* indicate a 500-bp marker. (*A*) M9K cells. (*B*) Mouse parietal pleural tissue. (*C*) Primary human mesothelial cells from healthy donor.

RT-PCR on the human pleural malignant mesothelioma cell lines M9K (Figure 1A), mouse parietal pleural tissues (Figure 1B), and primary pleural mesothelial cells isolated from human pleural fluid (Figure 1C). α and γ ENaC mRNAs were abundantly expressed in these samples. In contrast, β ENaC mRNA was detected at a lower expression level. Interestingly, two isoforms of δ ENaC were found in M9K, mouse pleural tissues, and human primary pleural mesothelial cells, identical to our previous observations in H441 cells, a human lung epithelial cell line (10). These results indicate that four ENaC subunits are expressed in human mesothelial cells at the steady-state mRNA level.

Indirect Immunofluorescent Detection of ENaC Proteins in Human Primary Mesothelial Cells and M9K Cells

Next, to detect α, β, γ, and δ ENaC subunit expression at the protein level, primary human mesothelial cells grown on coverslips were immunostained with specific anti-α, -β, -γ, and -δ ENaC antibodies. H441 monolayer cells were used as positive controls (10). To directly compare the ENaC expression in human primary mesothelial cells with those in H441 cells, M9K and human primary mesothelial cells were processed in parallel to H441 cells using the same protocol. As shown in Figure 2, cells in which nonimmune IgG was substituted for the anti-ENaC antibody displayed only 4′,6-diamidino-2-phenylindole labeling of the nuclei. In contrast, α, β, γ, and δ ENaC proteins were recognized by the specific anti-ENaC antibodies in primary human mesothelial cells (Figure 2). ENaC proteins were expressed through entire cell bodies. Differences in fluorescence intensity may reflect variable expression level of individual ENaC subunits, in addition to differences in affinity between the ENaC antibodies. The shape and size of each cell was not identical, possibly due to differences in their stage of differentiation. These observations show that ENaC expression in the pleural mesothelial and malignant mesothelioma cells were similar to those in H441 cells, as previously reported (10).

We also examined the distribution of ENaC subunits in M9K cells. As shown in Figures 3A and 3B, M9K cells plated on permeable supports and coverslips exhibited both green immunofluorescence, corresponding to α, β, γ, and δ ENaC expression in these cells, and blue immunofluorescence at the center, corresponding to cell nuclei. Furthermore, side view of confluent M9K monolayer showed that ENaC protein was expressed in the luminal side (Figure 3C). Similar results were seen in H441 cells (data not shown). These immunofluorescence data suggest that α, β, γ, and δ ENaC subunits are expressed in primary human mesothelial and mesothelioma cells at the protein level.

Western blot analysis of ENaC protein expression in M9K cells. H441 cells have been well documented as a model system for studying epithelial Na^+ channels (30, 31). Western blot analysis of cell extracts specifically detected polypeptides corresponding to α, γ, and δ ENaC subunits in H441 and M9K mesothelioma cells at 85 kD (Figure 4, left panel). Two bands were detected for α ENaC in M9K cells, which may be due to post-translational modification of ENaC proteins. These polypeptides were not detected when the the anti-ENaC antibodies were preincubated with an excess of immunogenic peptide (Figure 4, right panel).

Amiloride sensitivity of I_{sc} in confluent M9K monolayers and mouse parietal pleural tissues. Amiloride is a specific ENaC inhibitor with a concentration producing 50% inhibition (IC_{50}) of approximately 100 nM for highly selective native epithelial Na^+ channels and heterologously expressed αβγ ENaC channels (10, 15, 30). Conversely, some native Na^+ channels, two ENaC subunit channels (αβ and αγ), and δ ENaC–containing channels are less sensitive to amiloride (10, 11, 13, 14). To explore the functional expression of ENaC at the tissue level, amiloride-blockable transmesothelial I_{sc} were recorded across confluent M9K monolayers and mouse parietal pleural tissues while mounted in Ussing chambers. Typical I_{sc} current trace showing inhibition by different concentrations of amiloride (1 μM to 1 mM) in M9K-permealized monolayers are shown in Figure 5A. An IC_{50} value of 68 μM was obtained by fitting the concentration–effect relationship for amiloride (Figure 5B, $n = 3$). Similarly, amiloride could decrease I_{sc} dose dependently in mouse pleural tissues, and the IC_{50} value was 133 μM (Figures 5C and 5D, $n = 6$).

Heterologously Expressed αβγδ ENaC Channels in *Xenopus* Oocytes

To answer the question as to whether four ENaC subunits—namely, α, β, γ, and δ ENaC—expressed in human pleural mesothelial and malignant pleural mesothelioma cells can function as a cation-permeable channel, we coexpressed them in a well established expression system: *Xenopus* oocytes. Whole-cell, amiloride-sensitive currents after expression of αβγδ hENaC in oocytes are shown in Figure 6. Oocytes were initially perfused with ND-96 medium. The bath solution was then switched to ND-96 medium plus 10 μM amiloride, which immediately blocked approximately 90% of the currents in αβγδ hENaC–expressing oocytes. The blockade of amiloride was reversible. The total currents were restored after washing out the drug. The application of amiloride could be repeated several times on the same oocytes ($n = 4$), whereas no inhibitory effects of amiloride was

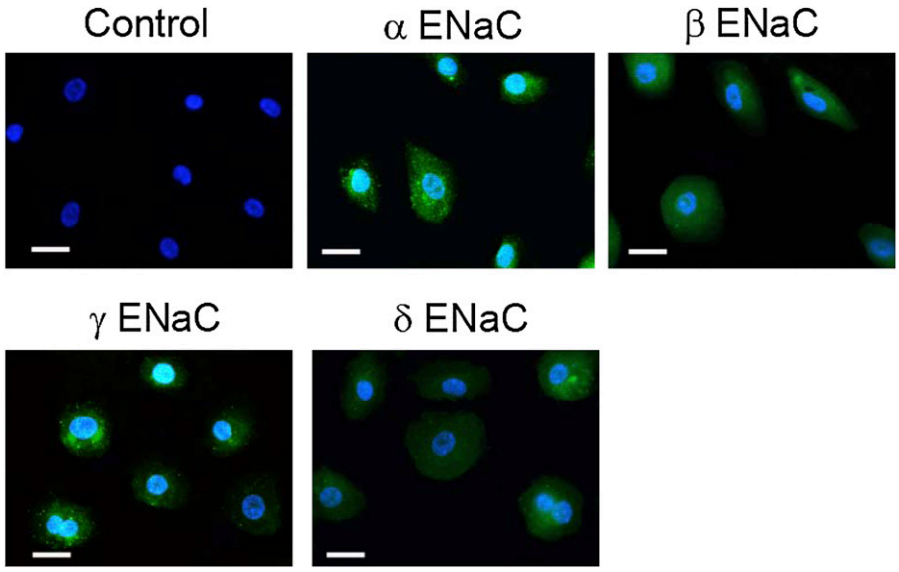

Figure 2. Immunofluorescent detection of ENaC proteins in human primary mesothelial cells. These images are representative of 10 similar fields from 3 independent experiments. Primary human mesothelial cells grown on coverslips were incubated with specific antibodies against α, β, γ, and δ ENaC subunits. ENaC antibodies were detected (*green channel*) with Alexa Fluor 488 goat anti-rabbit IgG (heavy + light). Nonimmune IgG was used to as negative control (*top left–most panel*). Cell nuclei were stained with 4′,6-diamidino-2-phenylindole (*blue channel*). *Scale bars* = 20 μm.

seen in control cells (Figure 6A). On average, the total Na^+ currents (ND-96) of αβγδ hENaC and basal currents in uninjected oocytes, respectively, were −3,680.7 (± 430) nA and −379.0 (± 51) nA at −100 mV. Correspondingly, the amiloride-resistant currents (amiloride) were −387.1 (± 55) nA in ENaC-injected oocytes and −336.9 (± 47) nA in control cells. There is a significant difference in the amiloride-sensitive Na^+ currents of αβγδ hENaC expressing oocytes and controls (Figure 6B) ($P <$

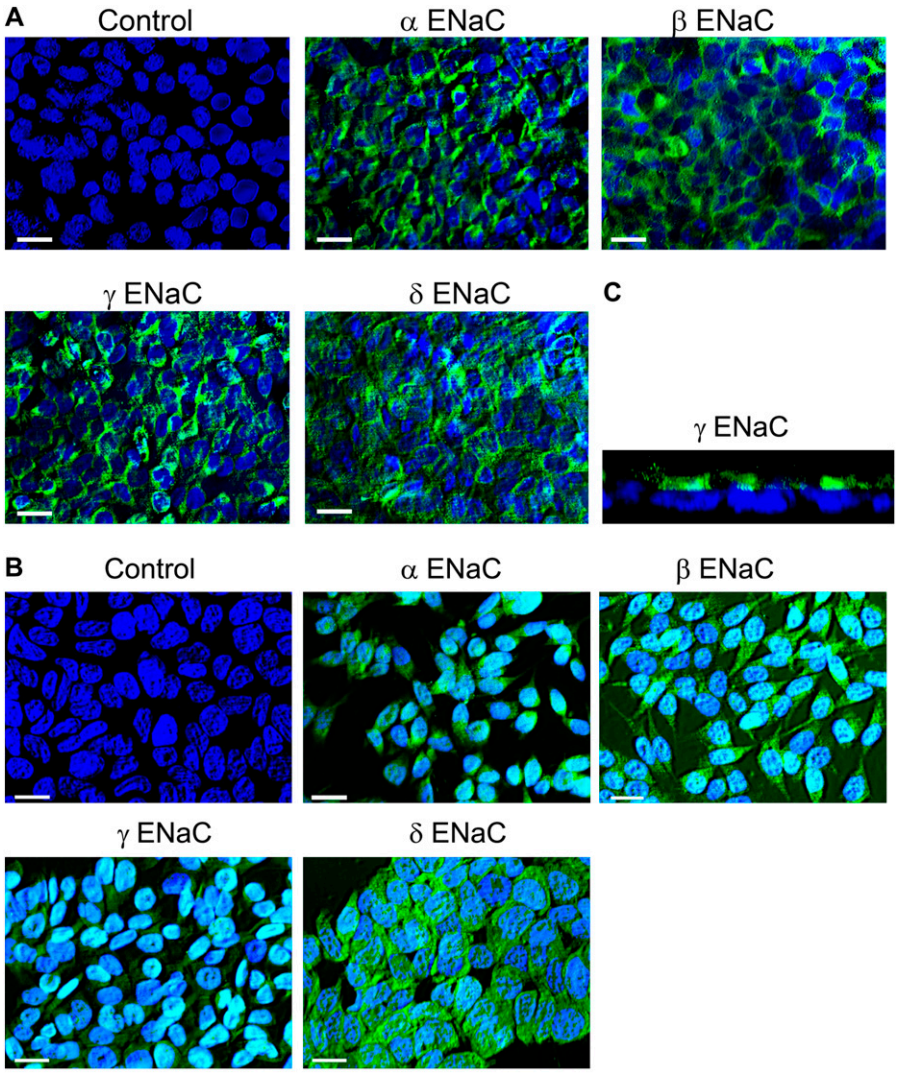

Figure 3. Immunofluorescent detection of ENaC proteins in confluent and unconfluent M9K malignant mesothelioma cells grown on permeable Transwell filter supports and coverslips. (*A*) Confluent M9K cells grown on permeable Transwell filters. Please *see* MATERIALS AND METHODS and the legend for Figure 2 for details. (*B*) M9K cells grown on coverslips. These images represent 10 similar results of 3 independent experiments. *Scale bars* = 20 μm. (*C*) Side view of confluent M9K monolayer using confocal microscopy.

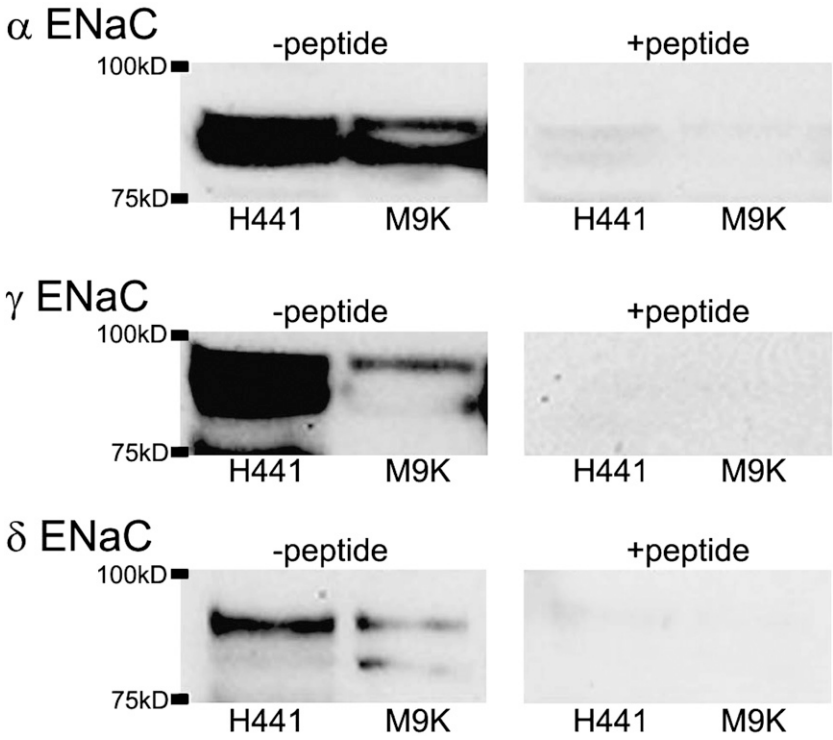

Figure 4. Western blot of ENaC proteins in M9K Cells. Proteins were extracted from M9K cells. H441 cells were used as a positive control. Blots were incubated with specific antibodies against α, γ, and δ ENaC subunits (*left panels*). To demonstrate specificity, the blots were incubated with the ENaC antibodies in the presence of an excess of the corresponding immunizing peptides (*right panels*). These experiments were repeated three times with identical results.

0.01; n = 8–10). Typically, amiloride-sensitive currents detected in control oocytes at −100 mV were close to the level of background noise, whereas macroscopic amiloride-sensitive currents produced by the αβγδ hENaC were from −3,694.9 to 928 nA (Figure 6C). Figure 6D shows the I-V curve of whole-cell currents at V_m from −120 mV to +80 mV. The I-V curve for the amiloride-sensitive Na^+ currents was nearly linear in the range of −120 to +80 mV, consistent with the electrophysiological properties of the ENaC channels. Resting V_ms were also recorded in oocytes expressing αβγδ hENaC (3.0 ± 0.2 mV; n = 10) and control oocytes (−18.0 ± 0.5 mV; n = 11) (Figure 6E). Overexpression of ENaC markedly depolarized the resting V_m due to cytosolic accumulation of Na^+ ions ($P < 0.01$).

Amiloride Sensitivity of Whole-Cell Na^+ Currents in Single M9K Cells

Our Ussing chamber studies suggest that a native ENaC-like channel is functionally expressed in human and mouse pleural mesothelial cells (Figure 5). To further characterize this channel biophysically, we performed whole-cell patch clamp studies using M9K cells. Figure 7A shows representative recordings of whole-cell currents in the presence of amiloride, ranging from 0 to 1,000 μM in one M9K cell. Amiloride reduced the currents, particularly the inward currents, in a dose-dependent manner. To compute the IC_{50} for amiloride, a dose–response curve was plotted with the whole-cell currents measured at −40 mV (Figure 7B). An IC_{50} value of 12 μM for amiloride was calculated when the experimental data were fitted with the Hill equation. In contrast, even the maximum dose of DMSO used for dissolving amiloride had no effect (data not shown).

External Na^+ affinity of the Na^+ channels in M9K cells. Extracellular Na^+ ions bind to ENaC proteins with a high affinity rate (32). To examine if the channel expressed in M9K cells exhibits high Na^+ affinity, as previously reported for native and cloned ENaC channels (32, 33), we perfused voltage-clamped M9K cells with bath solutions containing 0, 10, 30, 60, 100, and 140 mM Na^+ ions. As shown in Figure 8A, starting from Na^+-free bath medium, the whole-cell current gradually increased at −100 mV from −200 pA to −1,500 pA at the end of recording (140 mM Na^+). Current amplitudes measured at a given external Na^+ concentration were normalized to the one at 140 mM Na^+ ions and plotted as a function of bath Na^+ concentrations (Figure 8B). By fitting the plot with the Michaelis-Menten equation, the half-saturation constant (K_m) of 52.85 (± 11.47) mM for external Na^+ ions binding to the channel proteins was calculated (n = 4).

Cation Permeability

Three subtypes of native ENaC channels have been identified in lung epithelial cells (34). These channels exhibit divergent ion selectivity. Intriguingly, subunit composition of heterologously expressed ENaC channels is a key determinant of channel properties, including their permeability to cations (11). For example, the δβγ ENaC channel is much more permeable to Na^+ than Li^+ ions, whereas the opposite is true of αβγ ENaC (10, 13, 14). To examine whether the ENaC channels in M9K cells behave as αβγ- or δβγ-like channels, we determined the ion selectivity using the whole-cell mode. Replacement of Na^+ in the bath with Li^+ slightly increased the inward amiloride-sensitive Na^+ currents of M9K cells (Figure 9). The current density recorded in Li^+-containing external solution at −100 mV increased to −6.5 (± 2.0) pA/pF from that in Na^+-containing external solution (−5.2 ± 0.4 pA/pF; n = 5). On the other hand, consequent substitution of external Na^+ with K^+ markedly decreased the inward amiloride-sensitive Na^+ current density to −1.6 (± 0.3) pA/pF at −100 mV (n = 5). The relative permeability ratio of these cations was Li^+:Na^+:K^+ = 1.3:1.0:0.3. Figure 9A shows a typical step current trace recorded when perfused with Na^+, Li^+, and K^+ ions. Figure 9B shows the current–voltage relationships of whole-cell currents at V_m from −120 to +60 mV. The reversal potentials for Na^+, Li^+, and K^+ ions were +5.3, +4.1, and −10.9 mV, respectively. The I-V curves for amiloride-sensitive Na^+ currents associated with measured cations were nearly linear in the range −120 to 0 mV, a hallmark of ENaC

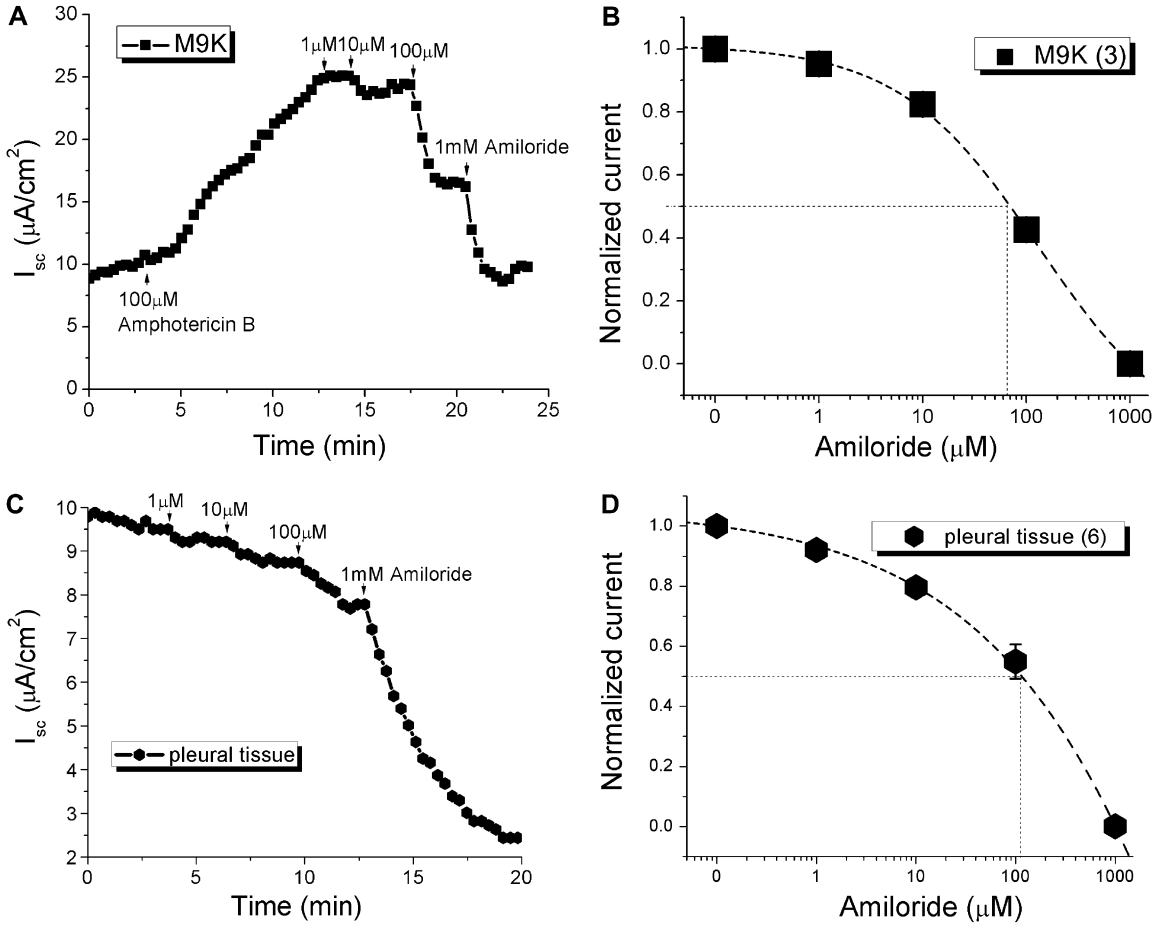

Figure 5. Amiloride blockade of short-circuit currents (I_{sc}s) in basolaterally permeabilized M9K monolayers and normal mouse pleural tissue. Transepithelial I_{sc}s were recorded with an Ussing chamber setup. (*A*) Typical current trace of I_{sc}. In this case, the apical compartment contained 145 mM Na^+, whereas the basolateral compartment contained 120 mM *N*-methyl-D-glucamine and 25 mM Na^+. Once a stable baseline was reached, 100 μM amphotericin B was added to the basolateral compartment, which resulted in increased I_{sc}. Amiloride (1–1,000 μM) was then added to the apical compartment (*arrow*). (*B*) Dose–response curve of amiloride blockade in M9K cells. Normalized amiloride-sensitive (AS) currents were calculated as follows: $I_{normalized} = 1 - (I_0 - I_\times)/(I_0 - I_{1,000})$, where I_0 is control value, $I_\times$ is steady-state current with concentration x, and $I_{1,000}$ is current measured with 1 mM amiloride. Values are means (± SE); numbers in *brackets* are samples recorded. The concentration producing 50% inhibition (IC_{50}) was calculated by best fit of data points to the following equation: $I_{normalized} = 1 + (x/IC_{50})^{coefficient}$. (*C*) Representative I_{sc} trace showing inhibition by different concentrations of amiloride in mouse pleural tissue. (*D*) The IC_{50} calculation method is the same as that described in (*B*).

channels. The whole-cell conductances (macroscopic conductance) calculated by fitting the I-V curves with a linear regression from −120 to 0 mV were 0.05 (± 0.002) nS for for Na^+ ions, 0.06 (± 0.002) nS for Li^+ ions, and 0.02 (± 0.001) nS for K^+ ions.

Single-Channel Conductance

Figure 10A shows the typical single-channel current traces recorded at various V_ms, which exhibited long open and closed times of, usually, several hundred milliseconds. This is a well-known characteristic of ENaC channel gating kinetics (30). The unitary current amplitudes were measured with CLAMPFIT, and a single-channel current–voltage plot was generated (Figure 10B). Single-channel conductance, obtained as a linear slope of the experimental data, was 15.4 pS for Li^+ ions. This result was similar to that documented in H441 cells (29).

Regulation of ENaC in Pleural Tissues by Cyclic AMP and Cyclic GMP

To understand the regulation of the amiloride-sensitive currents in pleural tissues by cyclic AMP (cAMP) and cyclic GMP (cGMP), we added 20 μM forskolin and 0.2 mM cGMP (8-pCPT-cGMP) to the mucosal bath of Ussing chambers. As shown in Figures 11A and 11B, the short-circuit Na^+ current across mouse pleural tissue was strikingly activated by forskolin and cGMP, which was inhibitable by amiloride, a specific inhibitor of ENaC. Interestingly, cGMP failed to activate the short-circuit Na^+ current in the presence of a protein kinase (PK) A inhibitor (Figure 11C). The I_{sc} level was raised to 1.75 (± 0.18)- and 1.96 (± 0.32)-fold by forskolin and cGMP compared with the basal current, respectively. Elevation of Na^+ transport via ENaC after the addition of forskolin and cGMP was statistically significant (Figure 11D; paired *t* test, $P < 0.05$; $n = 4$–7), whereas cGMP plus PKA inhibitor showed no obvious difference ($P > 0.05$; $n = 7$). Clearly, these observations show that ENaC channel activity in pleural tissues is stimulated by cyclic nucleotides.

DISCUSSION

Salt and fluid is continuously secreted into and cleared from the pleural space in mammals. The present, widely accepted concept with regard to pleural fluid is that the volume of pleural liquid

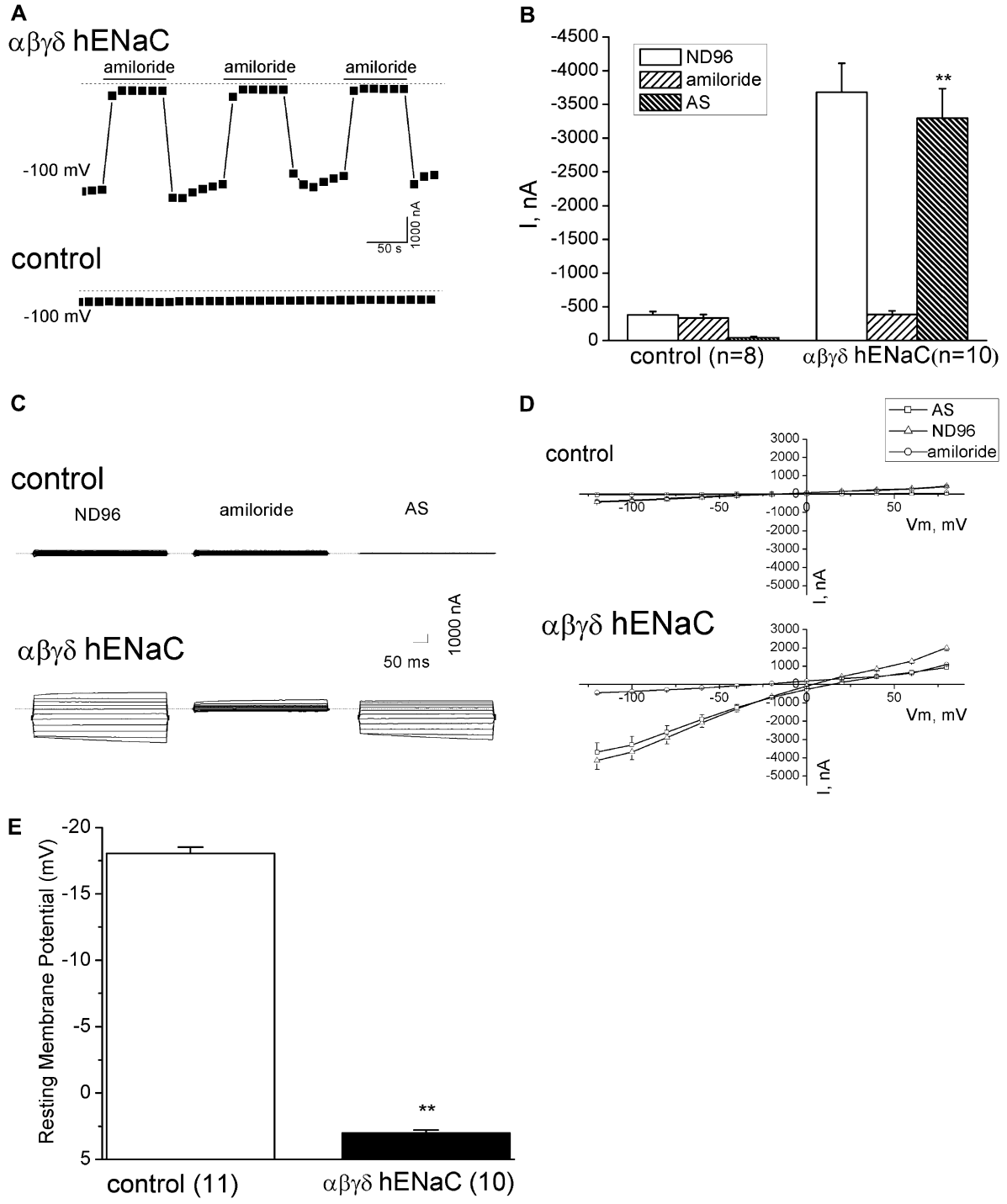

Figure 6. Whole-cell AS Na^+ currents in αβγδ human ENaC (hENaC)–expressing oocytes. AS currents were computed as the difference between the currents with and without 10 μM amiloride in the bath. (*A*) Representative whole-cell current recordings at −100 mV from an oocyte expressing αβγδ hENaC (αβγδ hENaC, *top panel*) and an uninjected oocyte (control, *bottom panel*). Oocytes were initially perfused with ND-96 medium. The bath solution was then switched to ND-96 medium plus 10 μM amiloride. This application of amiloride was repeated two additional times to the same oocyte, as indicted by *solid bars*. The *dashed lines* indicated zero current level. (*B*) Analysis of Na^+ currents (I) in uninjected (control) and αβγδ hENaC–expressing oocytes (αβγδ hENaC). ND-96, amiloride, and AS represent Na^+ currents recorded in ND-96 medium, ND-96 medium plus 10 μM amiloride, and subtraction of these two (AS currents), respectively. This result is consistent with (*A*) (*bottom*), showing that there are no AS Na^+ currents in uninjected oocytes. The number in *brackets* stands for the total oocytes for each group. $^{**}P < 0.01$, compared between AS of αβγδ hENaC and those of control. (*C*) Representative whole-cell Na^+ current traces before (ND-96, *left*) and after application of 10 μM amiloride (amiloride, *middle*) and their subtraction (AS, *right*) from an uninjected oocyte (control, *top*) and an oocyte expressing αβγδ hENaC (αβγδ hENaC, *bottom*). Oocytes were held at −40 mV, and then stepped from −120 mV to +80 mV in 20-mV increments. (*D*) Current–voltage relationships. Whole-cell Na^+ currents (I) at membrane potential (V_m) from −120 mV to +80 mV were recorded from an uninjected oocyte (control, *top*) and oocytes expressing αβγδ hENaC (αβγδ hENaC, *bottom*). Average current levels of total (ND-96, *triangle*), amiloride-resistant (Amiloride, *circle*), and AS Na^+ currents (AS, *square*) were plotted as a function of V_m. (*E*) Resting V_ms in oocytes expressing αβγδ hENaC (αβγδ hENaC) and uninjected cells (control). The number in *brackets* stands for the total oocytes for each group. $^{**}P < 0.01$.

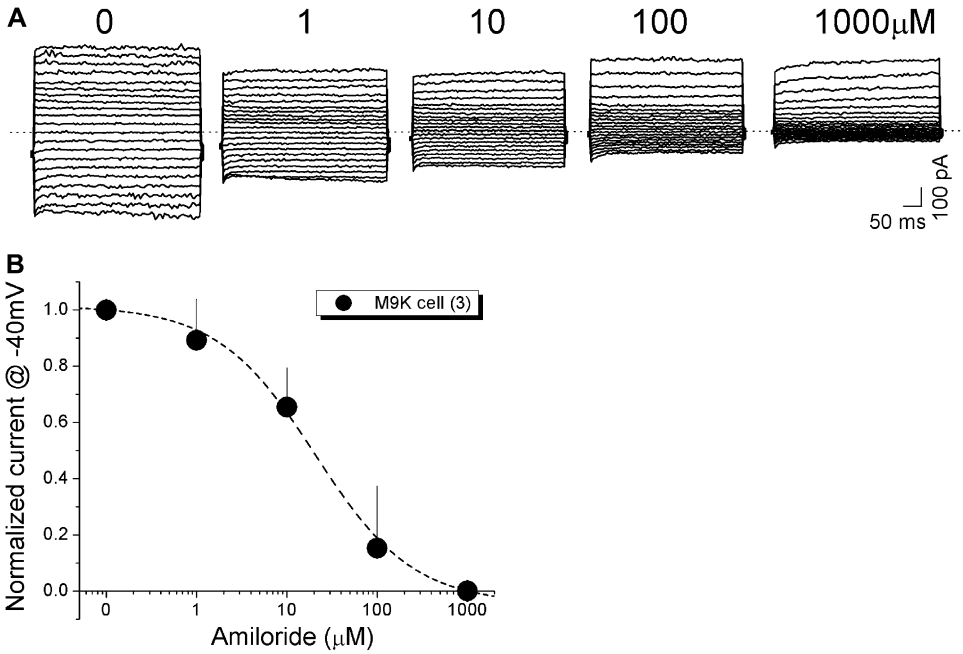

Figure 7. Patch clamp recordings of whole-cell currents and inhibition by amiloride in M9K cells. (*A*) Representative recordings of whole-cell currents and inhibition by different concentrations of amiloride (1 μM to 1 mM) in M9K cells. (*B*) Concentration-dependent inhibition of whole-cell currents by amiloride. For each cell, inward currents recorded at −40 mV were measured during perfusion with external solutions. IC_{50} was calculated by best fitting the raw data points to the Hill equation.

results from a balance of liquid in- and outflow, governed by Starling forces acting in the presence and absence of inflammation. Lymphatic drainage through amiloride-sensitive parietal pleura stomas, and electrolyte-coupled liquid absorption through the mesothelium of both sides, are major pathways for pleural fluid clearance (4, 35–37). A similar scenario exists in the context of malignant pleural mesothelioma, which is characterized by extravascular fibrin deposition, consistent with the aberrant fluid transport that characterizes most forms of solid neoplasia (38, 39). As abnormal fluid transport is implicated in the pathogenesis of pleural inflammation and neoplasia, we designed this study to incorporate analyses of both pleural mesothelial tissues and cultures of pleural mesothelial and malignant mesothelioma cells. Our results, for the first time, clearly show that epithelial Na^+ channels are expressed in pleural mesothelial and malignant mesothelioma cells at the steady-state mRNA and protein levels. Furthermore, the biophysical properties of the channel in these cells, including ion permeability, amiloride sensitivity, Na^+ dependence, unitary conductance, and responses to cyclic nucleotides, conform to those of amiloride-inhibitable Na^+ channels. These observations suggest that ENaC in mesothelial or malignant mesothelioma cells may be a rate-limiting step for removing pleural fluid or perineoplastic fluids, respectively.

The expression pattern in human and mouse mesothelial cells is identical to that in H441 cells, a human Clara epithelial cell line (10). Our RT-PCR and immunoassays, including Western blot and immunofluorescence studies, show that four ENaC subunits—namely, α, β, γ, and δ ENaC—are expressed in human primary mesothelial cells and M9K cell lines. We were unable to examine β ENaC protein expression in cell lysates, due to the lack of an anti–β ENaC antibody suitable for Western blotting. Our data, demonstrating ENaC expression at the mRNA and protein levels, prompted us to examine the functional expression of ENaC in mesothelial cells. For the majority of the electrophysiological experiments, we used M9K cells as a model, as these cells are easy to grow and have stable, consistent biophysical properties.

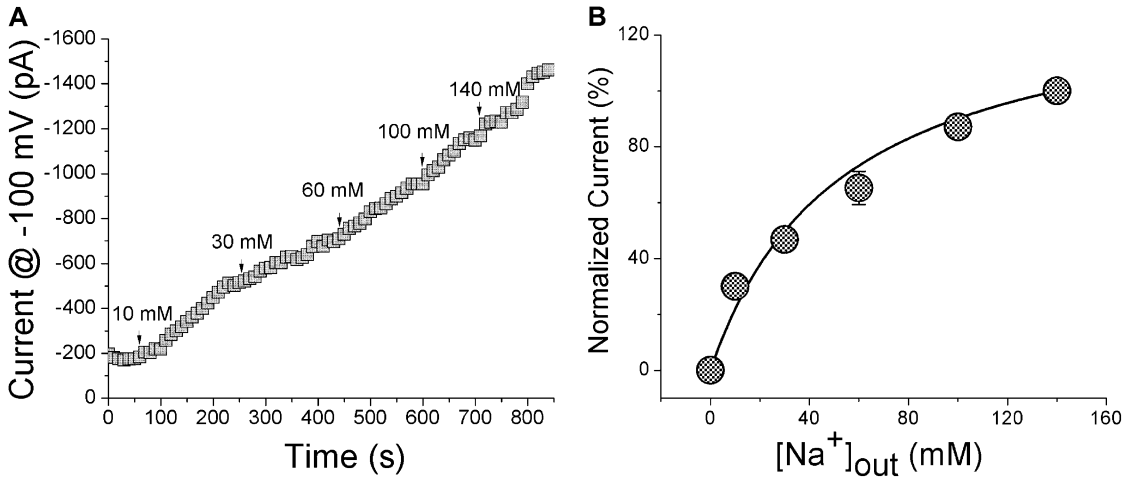

Figure 8. Na^+ affinity of native cation channels in M9K cells. (*A*) Typical traces recorded in the presence of varying concentrations of extracellular Na^+ ions. (*B*) Dependence of AS currents on bath Na^+ concentration ($[Na^+]_{out}$). Normalized currents were computed by dividing currents at D100 mV at the indicated $[Na^+]_{out}$ by the corresponding value at 140 mM Na^+; $n = 4$. *Solid line*: the raw data were fitted with the Michaelis-Menten equation (K_m: 52.85 ± 11.47 mM).

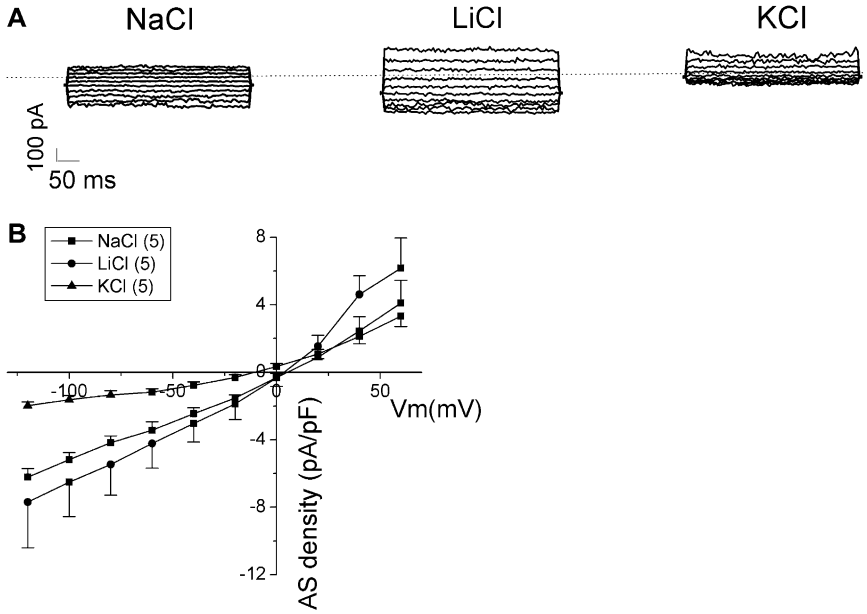

Figure 9. Cation selectivity of AS Na^+ channels in M9K cells. AS currents were computed by subtracting the whole-cell current obtained in the presence of 10 μM amiloride from the total current in the absence of drug. Measurements were conducted with external solutions predominately containing Na^+, Li^+, and K^+ ions as charge carriers. (*A*) Typical step current traces recorded when perfused with Na^+, Li^+, and K^+ ions. The *dashed lines* indicate zero current level. (*B*) Current–voltage relationships. Whole-cell AS current densities (AS density, pA/pF) at membrane potential (V_m, mV) from −120 mV to +60 mV were recorded from M9K cells. Average current levels in external solution containing Na^+ (*squares*), Li^+ (*circles*), or K^+ (*triangles*) ions were plotted as a function of V_m. Values are means (± SE). The number in *brackets* represents the total M9K cells for each group.

The differences in amiloride sensitivity observed between pleural tissues and single M9K cells can be explained by the voltage dependence of amiloride blockade, as described by several groups (14, 40–43). Amiloride carries a positive charge, and its binding site is located at the outer mouth of the channel pore, within the electrical field. It has been confirmed that the inhibitory efficiency of amiloride is less at depolarized V_ms (43). The holding potential for pleural tissues and M9K monolayer cells was 5 mV, whereas −100 mV was used for patch clamping single M9K cell. The difference in V_m between these two sets of experiments may result in differences in amiloride sensitivity. On the other hand, the value of IC_{50} for amiloride in single M9K cells is similar to that in oocytes expressing αβγδ hENaC and in H441 cells when clamped at the same potential, as previously described (10, 44).

Although culture conditions influence polarization of epithelial cells and, in turn, ion selectivity and amiloride inhibition (45, 46), this was not the case in our studies. Assuming mesothelial cells in pleural tissues and confluent M9K monolayers were well polarized, whereas M9K cells grown on coverslips were not, the IC_{50} value for amiloride in single M9K cells on coverslips should be greater. Contrary to this expectation, a smaller IC_{50} was obtained. It is intriguing that amiloride only exhibits its inhibitory effects on the native Na^+ channels in mesothelial cells when applied to the luminal side (equal to apical membrane of epithelial cells). These results strongly suggest that ENaC channels are expressed at the luminal side of mesothelial cells. Additional morphological studies dedicated to a separate project are needed to further locate their subcellular distribution.

In addition to the amiloride sensitivity, the results for external Na^+ affinity, single-channel conductance for Li^+ ions, and ion selectivity provide additional lines of evidence that ENaC-like channels are functionally expressed in pleural mesothelial and malignant mesothelioma cells. These biophysical features are consistent with the well characterized ENaC channels in H441 cells (29, 44).

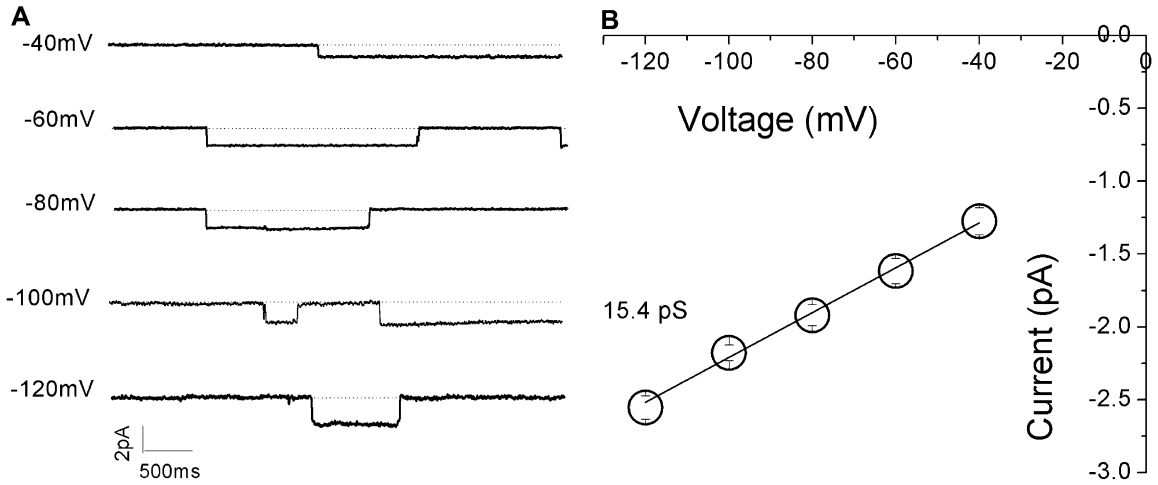

Figure 10. Single-channel recordings of Li^+-permeable channels in M9K cells. Cell-attached configuration was applied to record unitary currents at membrane potentials (V_ms) of −40 mV to −120 mV (from *top* to *bottom*). (*A*) Representative single-channel current traces. Closed level is indicated with *dotted lines*. One open level is shown. These experiments were repeated with M9K cells grown on glass coverslips for five passages. (*B*) Single-channel current–voltage relationship. Unitary current amplitudes were measured by CLAMPFIT from raw current traces. Average currents were plotted against V_ms. The Li^+ conductance was computed as the slope of the fitted linear line; $n = 6$.

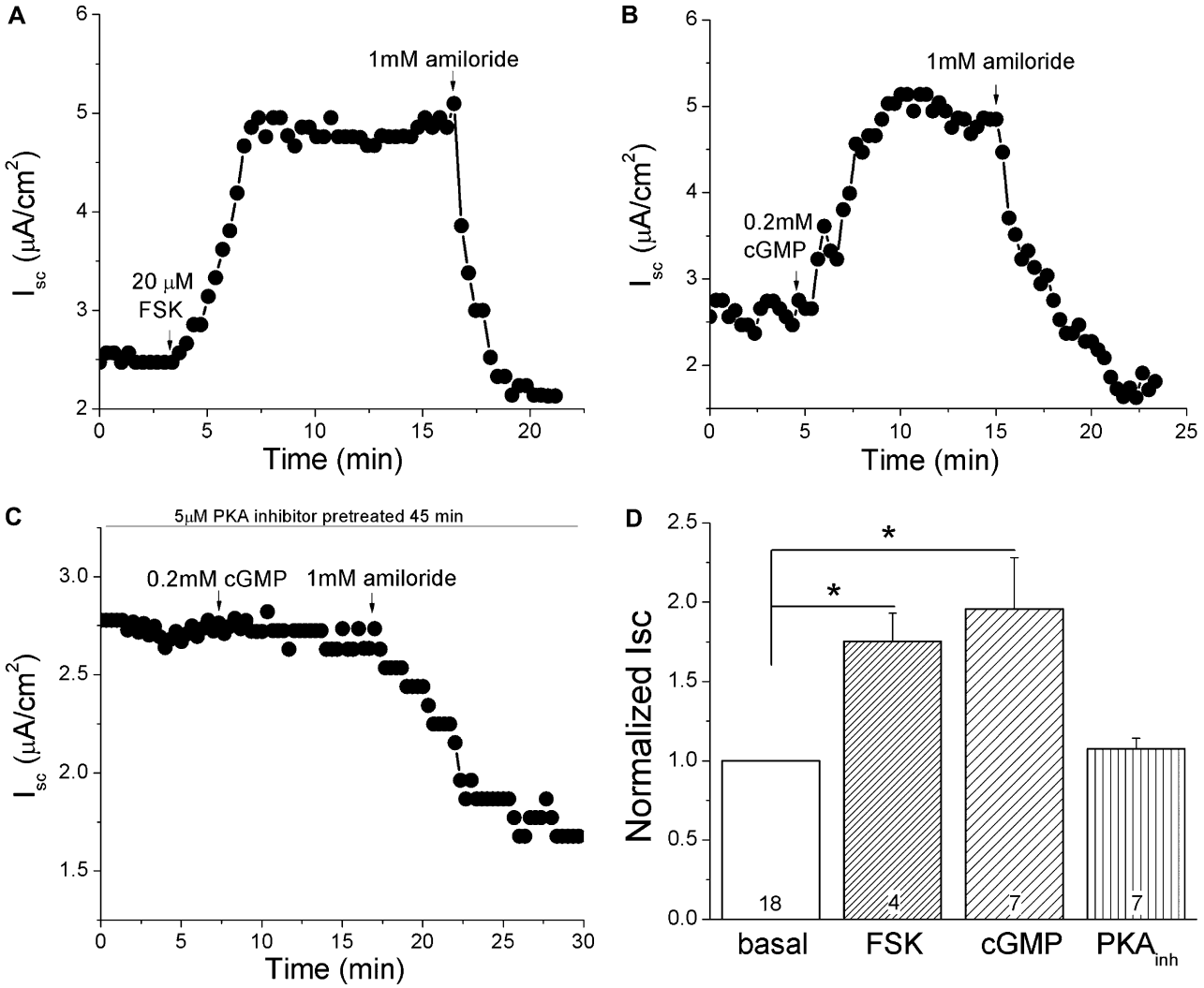

Figure 11. Regulation of transmesothelial I_{sc}s by cAMP and cGMP in mouse pleural tissues. Freshly excised pleural tissues from BALB/c male mice were mounted in horizontal Ussing chambers, as described in MATERIALS AND METHODS. Forskolin (20 μM), pCPT-cGMP salt (cGMP, 0.2 mM), and amiloride (1 mM) were added as indicated by *arrows*. (*A–C*) Representative I_{sc} trace in the presence of forskolin (FSK), cGMP, and cGMP plus protein kinase (PK) A inhibitor. (*D*) Normalized I_{sc} recorded in the absence (basal) and presence of forskolin (FSK), cGMP, and cGMP plus PKA inhibitor. Paired *t* test was used to analyze the statistical current differences between each drug by comparing the normalized current values before and after application to the bath. $*P < 0.05$; numbers are samples recorded.

Convincing evidence shows that native ENaC channels are regulated by PKA, PKC, and other kinases (25, 47). In this study, Ussing chamber assays showed that both forskolin and cell-permeable cGMP increased the amiloride inhibitable I_{sc}s in mouse pleural tissues. These results provide an intrinsic mechanism underlying the up-regulation of pleural or perineoplastic transmesothelial salt transport by cyclic nucleotides.

The combination of our biochemical, RT-PCR, and electrophysiological observations provides the first direct evidence of ENaC expression in pleural mesothelial cells/tissues and in malignant mesothelioma cells. Although we cannot completely exclude the association of amiloride-sensitive current with other amiloride-sensitive transport mechanisms in mesothelial or malignant mesothelioma cells (i.e., nucleotide-gated ion channels and electrogenic Na^+/Ca^{2+} exchangers), the ion selectivity, single-channel conductance, and amiloride sensitivity argue against this possibility.

Pleural effusions are commonly encountered in inflammatory and neoplastic clinical disorders, and result from the imbalance between pleural liquid turnover and reabsorption (48). Pleural effusion occurs in many diseases, including parapneumonic effusions, tuberculosis, and malignant pleural mesothelioma (49). Nucleotide-stimulated ENaC channels in human mesothelial cells may govern pleural fluid transport in the pleural cavity in normalcy, inflammatory disorders, and in pleural malignancy, and thereby contribute to homeostatic control of pleural fluid or the pathogenesis of pleural effusions. Whether impairment of ENaC occurs in pleural injuries awaits follow-up studies.

Conflict of Interest Statement: None of the authors has a financial relationship with a commercial entity that has an interest in the subject of this manuscript.

Acknowledgments: The authors thank Cheng Lili, Kathy Koenig, and Amy Tvinnereim for their superb technical assistance.

References

1. Lai-Fook SJ. Pleural mechanics and fluid exchange. *Physiol Rev* 2004;84: 385–410.
2. Nie HG, Tucker T, Su XF, Smith PR, Idell S, Ji HL. Electrolyte and fluid transport in mesothelial cells. *J Epithel Biol Pharmacol* 2008;1:1–7.

3. Yung S, Li FK, Chan TM. Peritoneal mesothelial cell culture and biology. *Perit Dial Int* 2006;26:162–173.
4. Zocchi L. Physiology and pathophysiology of pleural fluid turnover. *Eur Respir J* 2002;20:1545–1558.
5. Mutsaers SE. The mesothelial cell. *Int J Biochem Cell Biol* 2004;36:9–16.
6. Agostoni E, Zocchi L. Solute-coupled liquid absorption from the pleural space. *Respir Physiol* 1990;81:19–27.
7. Zocchi L, Agostoni E, Cremaschi D. Electrolyte transport across the pleura of rabbits. *Respir Physiol* 1991;86:125–138.
8. Canessa CM, Schild L, Buell G, Thorens B, Gautschi I, Horisberger JD, Rossier BC. Amiloride-sensitive epithelial Na^+ channel is made of three homologous subunits. *Nature* 1994;367:463–467.
9. Matthay MA, Robriquet L, Fang X. Alveolar epithelium: role in lung fluid balance and acute lung injury. *Proc Am Thorac Soc* 2005;2:206–213.
10. Ji HL, Su XF, Kedar S, Li J, Barbry P, Smith PR, Matalon S, Benos DJ. Delta-subunit confers novel biophysical features to alpha beta gamma-human epithelial sodium channel (ENaC) via a physical interaction. *J Biol Chem* 2006;281:8233–8241.
11. Fyfe GK, Canessa CM. Subunit composition determines the single channel kinetics of the epithelial sodium channel. *J Gen Physiol* 1998; 112:423–432.
12. Eaton DC, Chen J, Ramosevac S, Matalon S, Jain L. Regulation of Na^+ channels in lung alveolar type II epithelial cells. *Proc Am Thorac Soc* 2004;1:10–16.
13. Waldmann R, Champigny G, Bassilana F, Voilley N, Lazdunski M. Molecular cloning and functional expression of a novel amiloride-sensitive Na^+ channel. *J Biol Chem* 1995;270:27411–27414.
14. Ji HL, Bishop LR, Anderson SJ, Fuller CM, Benos DJ. The role of Pre-H2 domains of alpha- and delta-epithelial Na^+ channels in ion permeation, conductance, and amiloride sensitivity. *J Biol Chem* 2004;279:8428–8440.
15. Kleyman TR, Cragoe EJ Jr. Amiloride and its analogs as tools in the study of ion transport. *J Membr Biol* 1988;105:1–21.
16. Kleyman TR, Cragoe EJ Jr. The mechanism of action of amiloride. *Semin Nephrol* 1988;8:242–248.
17. Stefanidis I, Liakopoulos V, Kourti P, Zarogiannis S, Poultsidi A, Mertems PR, Salmas M, Hatzoglou C, Gourgoulianis K, Molyvdas PA. Amiloride-sensitive sodium channels on the parietal human peritoneum: evidence by Ussing-type chamber experiments. *ASAIO J* 2007;53:335–338.
18. Zarogiannis S, Kourti P, Hatzoglou C, Liakopoulos V, Poultsidi A, Gourgoulianis K, Molyvdas PA, Stefanidis I. Influence of the sodium transport inhibition by amiloride on the transmesothelial resistance of isolated visceral sheep peritoneum. *Adv Perit Dial* 2005;21:5–8.
19. Zarogiannis S, Hatzoglou C, Stefanidis I, Ioannou M, Paraskeva E, Gourgoulianis K, Molyvdas PA. Comparison of the electrophysiological properties of the sheep isolated costal and diaphragmatic parietal pleura. *Clin Exp Pharmacol Physiol* 2007;34:129–131.
20. Jiang J, Hu J, Bai C. Role of aquaporin and sodium channel in pleural water movement. *Respir Physiol Neurobiol* 2003;139:83–88.
21. Sakuma T, Folkesson HG, Suzuki S, Okaniwa G, Fujimura S, Matthay MA. β-Adrenergic agonist stimulated alveolar fluid clearance in *ex vivo* human and rat lungs. *Am J Respir Crit Care Med* 1997;155:506–512.
22. Sartori C, Fang X, McGraw DW, Koch P, Snider ME, Folkesson HG, Matthay MA. Selected contribution: long-term effects of β_2-adrenergic receptor stimulation on alveolar fluid clearance in mice. *J Appl Physiol* 2002;93:1875–1880.
23. Nie HG, Tucker T, Su XF, Smith PR, Idell S, Ji HL. Expression of four ENaC subunits in human mesothelial cells. *Am J Respir Crit Care Med* 2008;177:A800.
24. Jiang Y, Cong P, Williams SR, Zhang W, Na T, Ma HP, Peng JB. WNK4 regulates the secretory pathway via which TRPV5 is targeted to the plasma membrane. *Biochem Biophys Res Commun* 2008;375:225–229.
25. Woollhead AM, Scott JW, Hardie DG, Baines DL. Phenformin and 5-aminoimidazole-4-carboxamide-1-beta-D-ribofuranoside (AICAR) activation of AMP-activated protein kinase inhibits transepithelial Na^+ transport across H441 lung cells. *J Physiol* 2005;566:781–792.
26. Guo Y, DuVall MD, Crow JP, Matalon S. Nitric oxide inhibits Na^+ absorption across cultured alveolar type II monolayers. *Am J Physiol* 1998;274:L369–L377.
27. Thome UH, Davis IC, Nguyen SV, Shelton BJ, Matalon S. Modulation of sodium transport in fetal alveolar epithelial cells by oxygen and corticosterone. *Am J Physiol Lung Cell Mol Physiol* 2003;284:L376–L385.
28. Voilley N, Lingueglia E, Champigny G, Mattei MG, Waldmann R, Lazdunski M, Barbry P. The lung amiloride-sensitive Na^+ channel: biophysical properties, pharmacology, ontogenesis, and molecular cloning. *Proc Natl Acad Sci USA* 1994;91:247–251.
29. Itani OA, Auerbach SD, Husted RF, Volk KA, Ageloff S, Knepper MA, Stokes JB, Thomas CP. Glucocorticoid-stimulated lung epithelial Na(+) transport is associated with regulated ENaC and sgk1 expression. *Am J Physiol Lung Cell Mol Physiol* 2002;282:L631–L641.
30. Lazrak A, Matalon S. cAMP-induced changes of apical membrane potentials of confluent H441 monolayers. *Am J Physiol Lung Cell Mol Physiol* 2003;285:L443–L450.
31. Shlyonsky V, Goolaerts A, Van Beneden R, Sariban-Sohraby S. Differentiation of epithelial Na^+ channel function: an *in vitro* model. *J Biol Chem* 2005;280:24181–24187.
32. Lazrak A, Samanta A, Matalon S. Biophysical properties and molecular characterization of amiloride-sensitive sodium channels in A549 cells. *Am J Physiol Lung Cell Mol Physiol* 2000;278:L848–L857.
33. Inagaki A, Yamaguchi S, Ishikawa T. Amiloride-sensitive epithelial Na^+ channel currents in surface cells of rat rectal colon. *Am J Physiol Cell Physiol* 2004;286:C380–C390.
34. Matalon S, Benos DJ, Jackson RM. Biophysical and molecular properties of amiloride-inhibitable Na^+ channels in alveolar epithelial cells. *Am J Physiol* 1996;271:L1–L22.
35. Miserocchi G. Physiology and pathophysiology of pleural fluid turnover. *Eur Respir J* 1997;10:219–225.
36. Mitrouska I, Bouros D. The trans-exudative pleural effusion. *Chest* 2002; 122:1503–1505.
37. Wiener-Kronish JP, Albertine KH, Licko V, Staub NC. Protein egress and entry rates in pleural fluid and plasma in sheep. *J Appl Physiol* 1984;56:459–463.
38. Idell S, Pueblitz S, Emri S, Gungen Y, Gray L, Kumar A, Holiday D, Koenig KB, Johnson AR. Regulation of fibrin deposition by malignant mesothelioma. *Am J Pathol* 1995;147:1318–1329.
39. Dvorak HF. Tumors: wounds that do not heal: similarities between tumor stroma generation and wound healing. *N Engl J Med* 1986;315: 1650–1659.
40. Garty H, Benos DJ. Characteristics and regulatory mechanisms of the amiloride-blockable Na^+ channel. *Physiol Rev* 1988;68:309–373.
41. Kashlan OB, Sheng S, Kleyman TR. On the interaction between amiloride and its putative alpha-subunit epithelial Na^+ channel binding site. *J Biol Chem* 2005;280:26206–26215.
42. Kellenberger S, Gautschi I, Schild L. Mutations in the epithelial Na^+ channel ENaC outer pore disrupt amiloride block by increasing its dissociation rate. *Mol Pharmacol* 2003;64:848–856.
43. Segal A, Awayda MS, Eggermont J, Van Driessche W, Weber WM. Influence of voltage and extracellular Na^+ on amiloride block and transport kinetics of rat epithelial Na^+ channel expressed in *Xenopus* oocytes. *Pflugers Arch* 2002;443:882–891.
44. Ramminger SJ, Richard K, Inglis SK, Land SC, Olver RE, Wilson SM. A regulated apical Na^+ conductance in dexamethasone-treated H441 airway epithelial cells. *Am J Physiol Lung Cell Mol Physiol* 2004;287: L411–L419.
45. Kunzelmann K, Kathofer S, Hipper A, Gruenert DC, Gregner R. Culture-dependent expression of Na^+ conductances in airway epithelial cells. *Pflugers Arch* 1996;431:578–586.
46. Yue G, Hu P, Oh Y, Jilling T, Shoemaker RL, Benos DJ, Cragoe EJ Jr, Matalon S. Culture-induced alterations in alveolar type II cell Na^+ conductance. *Am J Physiol* 1993;265:C630–C640.
47. Bao HF, Zhang ZR, Liang YY, Ma JJ, Eaton DC, Ma HP. Ceramide mediates inhibition of the renal epithelial sodium channel by tumor necrosis factor-alpha through protein kinase C. *Am J Physiol Renal Physiol* 2007;293:F1178–F1186.
48. Medford A, Maskell N. Pleural effusion. *Postgrad Med J* 2005;81:702–710.
49. Russo P, Catassi A, Malacarne D, Margaritora S, Cesario A, Festi L, Mule A, Ferri L, Granone P. Tumor necrosis factor enhances SN38-mediated apoptosis in mesothelioma cells. *Cancer* 2005;103:1503–1518.